| OF |
AD
A053806

MICROCOPY RESOLUTION TEST CHART

OPTICAL-MICROWAVE INTERACTIONS IN SEMICONDUCTOR DEVICES

Huan-Wun Yen and Michael K. Barnoski

Hughes Research Laboratories

3011 Malibu Canyon Road

Malibu, CA 90265

April 1978

Approved for public release; distribution unlimited.

D D C
RECEIVED
MAY 11 1978
D

REPORT DOCUMENTATION PAGE	READ INSTRUCTIONS BEFORE COMPLETING FORM

Quarterly rept. no. 3, 17 Dec 77 - 17 Mar 78

1. REPORT NUMBER	2. GOVT ACCESSION NO.	3. RECIPIENT'S CATALOG NUMBER

4. TITLE (and Subtitle)	5. TYPE OF REPORT & PERIOD COVERED
Optical - Microwave Interactions In Semiconductor Devices	Quarterly Report 3 17 Dec 1977-17 March 1978
	6. PERFORMING ORG. REPORT NUMBER

7. AUTHOR(s)	8. CONTRACT OR GRANT NUMBER(s)
Huan-Wun Yen Michael K. Barnoski	N00173-77-C-0156

9. PERFORMING ORGANIZATION NAME AND ADDRESS	10. PROGRAM ELEMENT, PROJECT, TASK AREA & WORK UNIT NUMBERS
Hughes Research Laboratories 3011 Malibu Canyon Road Malibu, CA 90265	

11. CONTROLLING OFFICE NAME AND ADDRESS	12. REPORT DATE
Naval Research Laboratory 4555 Overlook Ave., S. W. Washington, D.C. 20375	April 1978
	13. NUMBER OF PAGES 42

37 p.

14. MONITORING AGENCY NAME & ADDRESS(if different from Controlling Office)	15. SECURITY CLASS. (of this report)
	Unclassified
	15a. DECLASSIFICATION DOWNGRADING SCHEDULE

16. DISTRIBUTION STATEMENT (of this Report)

Approved for public release; distribution unlimited.

17. DISTRIBUTION STATEMENT (of the abstract entered in Block 20, if different from Report)

18. SUPPLEMENTARY NOTES

19. KEY WORDS (Continue on reverse side if necessary and identify by block number)

GaAs IMPATT diode, Optical switching of IMPATT oscillator, small signal analysis, Microwave Cavity

20. ABSTRACT (Continue on reverse side if necessary and identify by block number)

Theoretical calculations were carried out to explain the observed results of optical switching of GaAs IMPATT diode oscillators. In the previous experiments it was found that depending on the diode's bias condition, the frequency of oscillation, and the intensity of illumination, the IMPATT microwave output power could be either

DD FORM 1473 1 JAN 73   EDITION OF 1 NOV 65 IS OBSOLETE

172 600

20. Abstract (Continued)

enhanced or reduced. This problem was treated by carrying out a
theoretical calculation of the property of IMPATT diode under optical
illumination. It was determined that the most significant contribu-
tion of optical illumination in an IMPATT diode is the drastic increase
in reverse saturation current I_s. Using small signal analysis we
obtained an expression for the total impedance of the IMPATT diode
under optical illumination. It was found that optical illumination
causes the shifting of the negative resistance and reactance versus
frequency curves. This in turn causes the oscillation frequency to
vary and the output power to drop in general. However, the cavity
tuning yields a strongly frequency dependent threshold for the diode.
Therefore under certain circumstance optical illumination can actually
trigger the IMPATT diode into oscillation also.

PREFACE

The following personnel contributed to the research work reported here: H. W. Yen, M. K. Barnoski, A. Yariv (consultant), and D. F. Lewis.

TABLE OF CONTENTS

LIST OF ILLUSTRATIONS

SECTION 1

INTRODUCTION AND SUMMARY

Optical photons with energies higher than the bandgap energy of a semiconductor can excite electron-hole pairs in that material. Although the characteristics of almost all semiconductor devices depend heavily on the number of charge carriers available, strong interactions between the device performance and the illuminating optical signal can be expected. The program "Optical-Microwave Interactions in Semiconductor Devices" is intended to study such interactions as manifested in the modification of characteristics of semiconductor microwave devices by optical illumination. Through an understanding of these interaction processes, we can explore some potential applications, such as optical switching and optical injection locking of solid-state oscillators, phase jitter and frequency drift reduction of oscillators by optical illumination, and optically injected microwave mixing in solid-state amplifiers.

During the third quarter of this program, we concentrated on the theoretical calculations of optical switching of GaAs IMPATT diode oscillators. We had previously experimentally studied the microwave oscillation characteristics of GaAs IMPATT diodes under external optical illumination. We had found that, depending on the diode's bias condition, the frequency of oscillation, and the intensity of illumination, the IMPATT microwave output power can be either enhanced or reduced. This result is described in more detail in Section 2. Section 3 presents a theoretical calculation of the properties of IMPATT diodes under optical illumination. We determined that the most significant contribution of optical illumination in an IMPATT diode is the drastic increase in reverse saturation current I_s. Under normal operation conditions I_s is due to thermally generated carriers and is negligible compared with the avalanche current. However, with intense optical illumination, I_s must be included in the dynamic equations that govern the operation of the device.

Using a small-signal approximation, equations can be solved to
show that optical illumination effectively introduces a resistance in
the equivalent circuit of the diode and that this resistance damps the
microwave oscillation and reduces the device efficiency and power output.
In an ordinary IMPATT diode, the cut-off frequency (the frequency at
which the real part of the impedance vanishes) and the resonant frequency
(the frequency at which the imaginary part of the impedance vanishes)
are identical. Under illumination, however, these two frequencies are
different. As shown in Section 4, this causes the interesting behavior
of the IMPATT oscillator that qualitatively agrees with experimental
observations.

During the past quarter, we also attempted to measure the noise
figure of a GaAs FET amplifier used as a mixer. However, the effort was
not successful because the amplifier used was not an efficient mixer.
The total loss of the mixing process is out of the noise-figure meter
sensitivity range. Currently, we are in the process of fabricating some
more FET amplifiers for more measurements.

SECTION 2

EXPERIMENTAL RESULTS OF OPTICAL SWITCHING OF GaAs
IMPATT DIODE OSCILLATOR

The basic principles and characteristics of IMPATT diodes have been described extensively in the literature.[1-3] The structure of these diodes can be regarded as consisting of two main sections, the avalanche region and the drift region. Under normal operation, the diodes are reverse biased into avalanche breakdown so that electron-hole pairs are generated in the avalanche region by impact ionization. The electrons then move across the drift region under the influence of the external electric field. Because of the time delay in the avalanche multiplication process and the drifting process, the device exhibits negative resistance at microwave frequencies. Electron-hole pairs can also be generated in a semiconductor by illumination with an optical beam of sufficient photon energy. Since carrier generation is the key to the operation of IMPATT diodes, a strong interaction between the optical beam and microwave output of the IMPATT diode is expected.

This section describes an experimental study of the effect of optical illumination on the IMPATT diode oscillation characteristics. The IMPATT diodes used in this experiment are GaAs Schottky-barrier junction diodes operating at about 16 GHz. The thickness of the active layer is ~ 2.8 μm, and the doping level is $N_d \sim 2 \times 10^{16}$ cm^{-3}. The diodes were mounted in a tuned microwave cavity with a feedthrough that allows an optical fiber to be butt-coupled to the active region of the diode as sketched in Figure 1. A sliding short waveguide section was connected to one side of the cavity to increase the frequency range of tuning. On the other side, a coupling probe and crystal detector was attached for the detection of microwave output. A cw GaAlAs laser and a pulsed GaAs laser were used as light sources. The output of the laser was coupled into the fiber and guided down to the IMPATT diode.
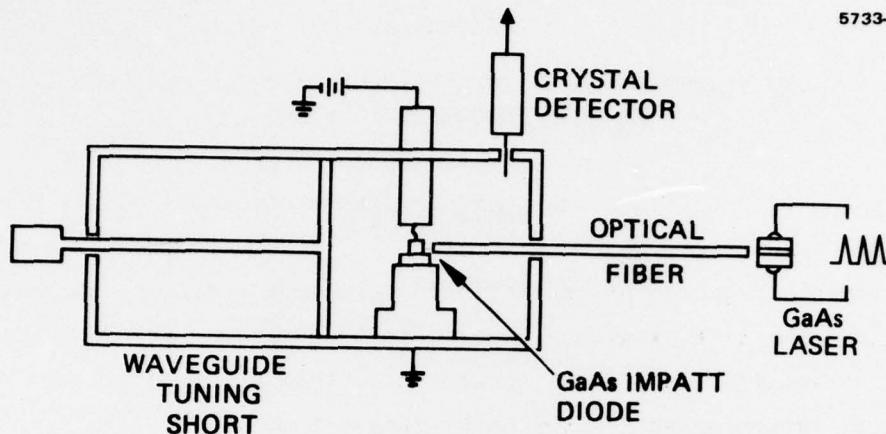
11

Figure 1. Schematic of the experimental setup.

Figure 2 shows the reverse bias current-voltage (I-V) characteristic of one of the IMPATT diodes. With no illumination, the diode had a reverse breakdown voltage of ∿30 V and a small leakage current. Illumination with 8200 Å light from a GaAlAs cw laser through a fiber produced a photocurrent, as shown in Figure 2(b). At voltages << $V_{breakdown}$, the photocurrent was approximately 75 μA for this diode; however, at 28 V, avalanche multiplication resulted in a total photocurrent of 160 μA. Other diodes exhibited a similar photoresponse. The optical power emitted from the fiber waveguide was measured to be ∿7 mW.

The pulse photoresponse of the IMPATT diodes was also investigated by using a GaAs laser source emitting a 100 to 150 nsec long pulse of ∿9000 Å light at a repetition rate of approximately 500 PPS. Several types of response were observed depending on the illumination intensity and the "state" of the diode, which includes the bias condition and the operation frequency. Figure 3 shows the photoresponse of an IMPATT diode which was biased above threshold. The cavity in this case was tuned to optimize the microwave output power. The upper trace in the pictures is the light pulse from the GaAs laser, and the lower trace is the dc voltage output of the crystal detector, which is proportional to the microwave power of the IMPATT diodes. The zero level for micro- wave power is as indicated on the picture. Figure 3(a) shows a decrease

12

5733-2
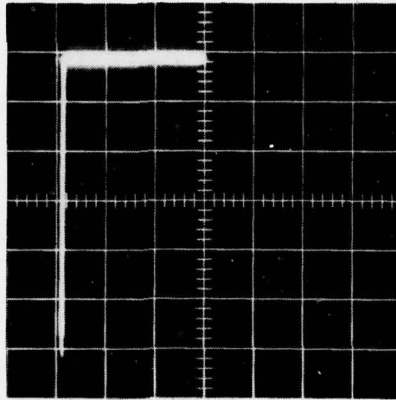
(a) Without laser light
   illumination.
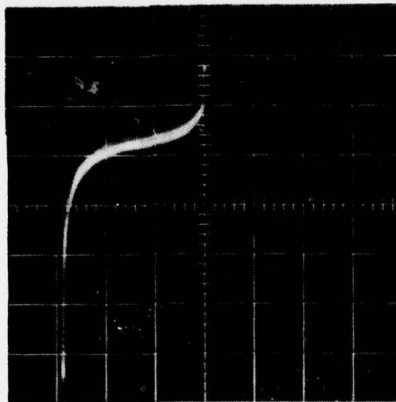
(b) With laser light
    illumination.

Figure 2.   IMPATT diode I-V
characteristics. (Horizon-
tal scale 10V/div, vertical
scale 50 μA/div.)

13

5733-3

ZERO MICROWAVE
POWER LEVEL

(a) At low light intensity.
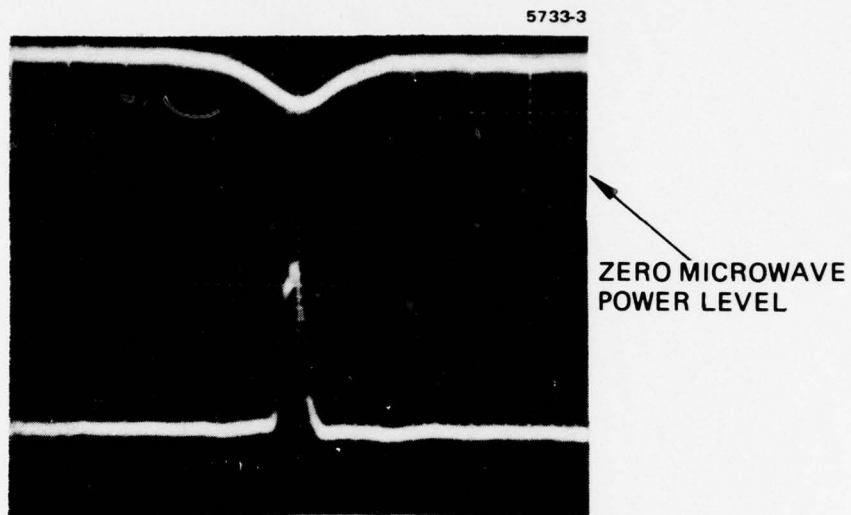
ZERO MICROWAVE
POWER LEVEL
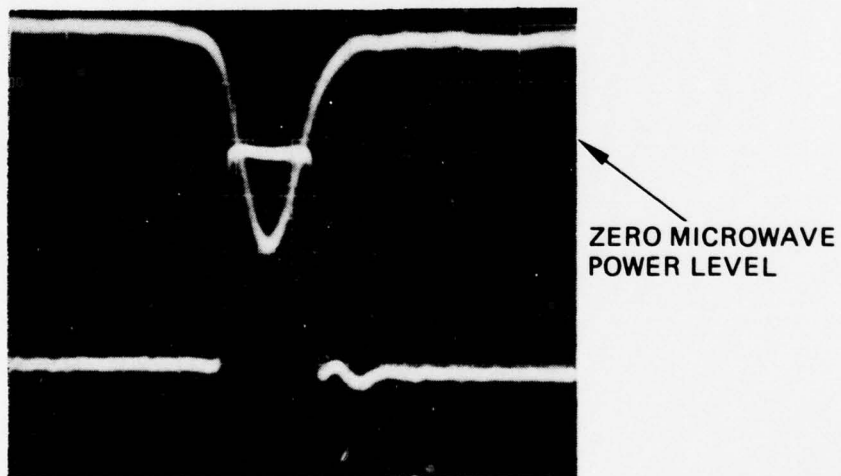
(b) At higher intensity.

Figure 3. Pulse photoresponse of GaAs IMPATT diode
biased above threshold. The upper trace is the
light pulse, the lower trace is the microwave output
power. (Horizontal scale 100 nsec/div.)

14

in the microwave power output during the duration of the light pulse. The peak reduction is about 60%. As the light intensity is increased, as shown in Figure 3(b), the IMPATT was nearly shut off for a time interval corresponding to the light pulse duration.

If the cavity is detuned slightly so that the cavity Q favors some other frequency of oscillation that has a higher threshold, the cw micro-wave power will be almost zero as shown in Figure 4(a). Illumination with a small light pulse in this case actually triggered the device into oscil-lation generating pulses of microwave output. This microwave output was very sensitive to the light intensity. A 10% increase in light intensity gave a 75% enhancement of microwave output, as seen in Figure 4(b). However, further increase in light intensity resulted in a situation shown in Figure 4(c) and 4(d). The microwave output enhancement was seen near the beginning of the light pulse but was quickly shut-off for as long as the light intensity was above a certain critical level. As the light intensity fell below this level, microwave output enhancement resumed.

If we start from the state shown in Figure 4(b) or 4(d) and increase the dc bias current we can obtain the situation shown in Figure 3(a) or 3(b). This is because, with sufficient bias current, the device operates close to its optimum condition. Then the only effect the light pulse has is to spoil this optimum.

Thus, we have observed a strong interaction between the optical pulse and the microwave oscillation characteristics of GaAs IMPATT diodes. Both microwave power reduction and enhancement were achievable depending on the bias condition and oscillation frequency of the device. In Sections 3 and 4, a simple theory based on the small-signal analysis is presented to explain the observed phenomena.
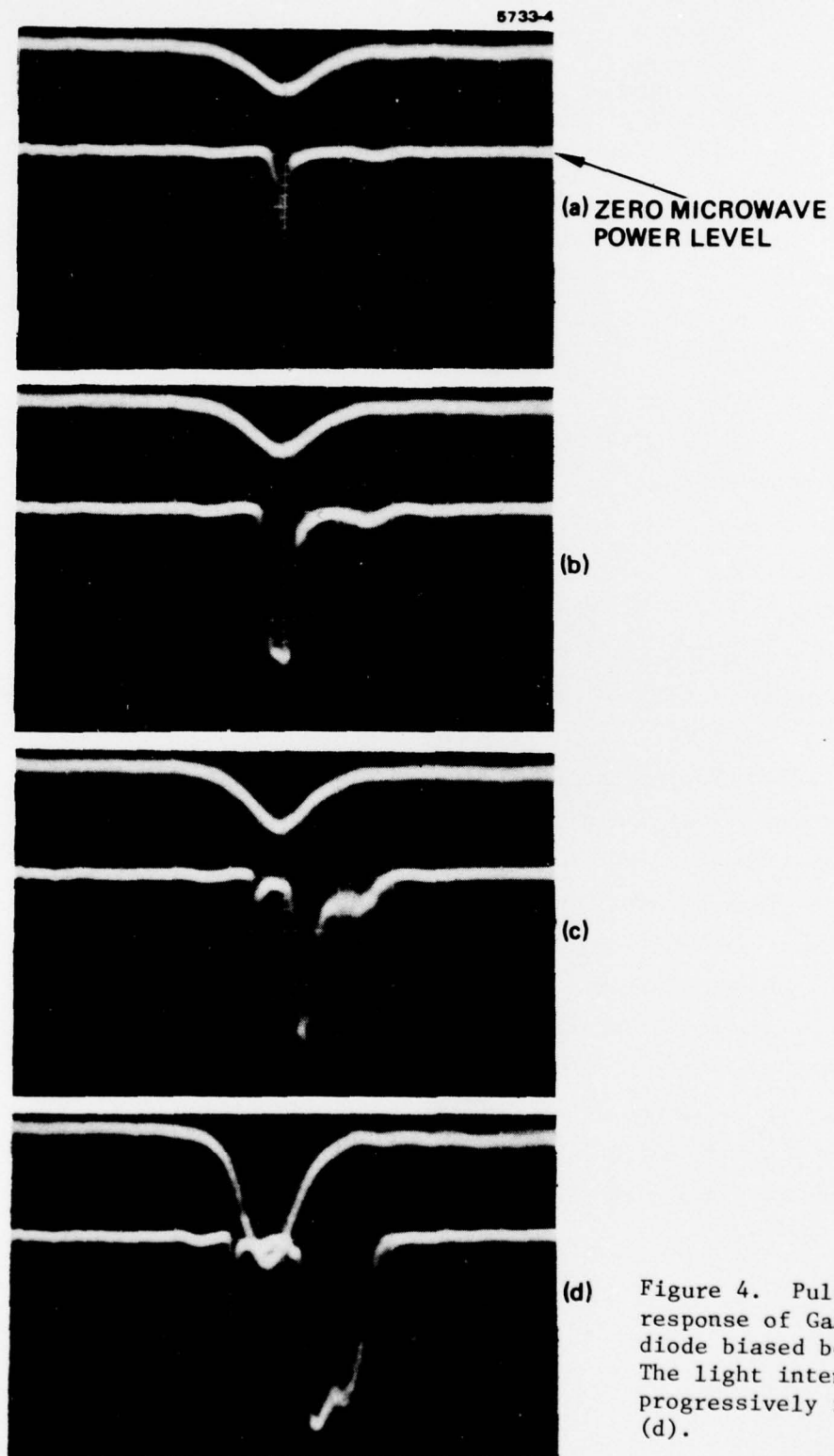
15

5733-4

(a) ZERO MICROWAVE POWER LEVEL

(b)

(c)

(d) Figure 4. Pulse photo-response of GaAs IMPATT diode biased below threshold. The light intensity increases progressively from (a) to (d).

SECTION 3

SMALL-SIGNAL ANALYSIS OF IMPATT DIODE CHARACTERISTICS
UNDER OPTICAL ILLUMINATION

To understand the results described in Section 2 requires studying the dependence of the device impedance on the various parameters, such as the dc bias current I_o, the oscillation frequency ω and the transit angle θ, and the optically generated current I_s.[5,6] The structure that we are going to study is shown in Figure 5, which is a typical abrupt p-n junction in reverse bias to break down. For analysis, we break the diode into two regions, the avalanche zone with length ℓ_a and the drift zone with length ℓ_d, as shown in Figure 5(a). Figure 5(b) depicts the electric field as a function of position inside the depletion zone. The electric field profile has a triangular shape, peaking near the p-n junction boundary, which corresponds to the avalanche zone.

In a typical avalanche diode, the peak electric field is estimated to be about 5×10^5 V/cm. Under this field, the carrier drift velocity of both holes and electrons is nearly identical with a value of 9×10^6 cm/sec. Since the carrier drift velocity is nearly uniform throughout the depletion zone, it is treated as a constant in the following calculations.

We will use a small-signal analysis to calculate the impedance of the diode in the avalanche zone and the drift zone separately. This is done by deriving expressions for the ac voltages in terms of the ac circuit current and thereby obtain the impedance.

A. THE AVALANCHE ZONE

Consider the avalanche zone first. The one-dimensional equation that describes the avalanche current as a function of time can be derived as follows:

$$\frac{\partial E}{\partial x} = \frac{q}{\varepsilon} (N_D^+ - N_A^- + p - n) \qquad \text{Poisson's equation}$$
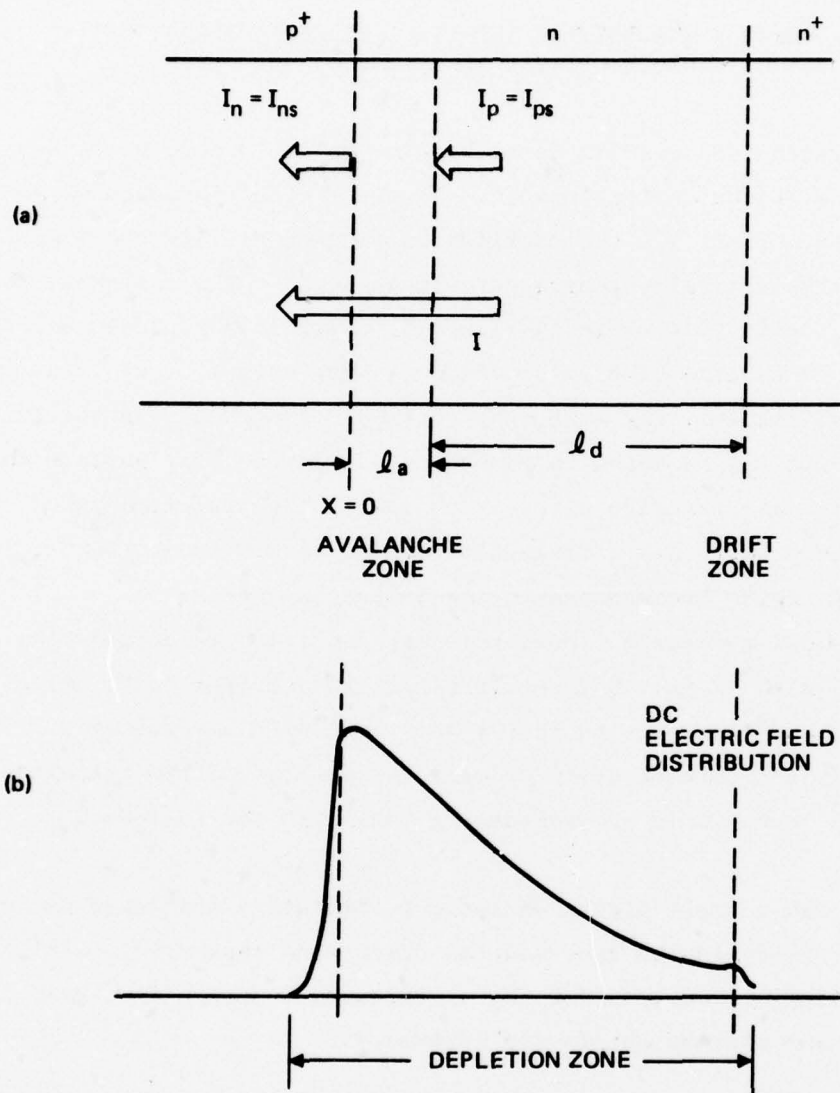
(a)

(b)

Figure 5. Structure of the IMPATT diode studied.

(a) Boundary conditions of the avalanche zone.

(b) Electric field distribution in the depletion
     zone of the diode.

18

$$I_n = qv_d nA$$

$$I_p = qv_d pA$$

$$I = I_n + I_p = qv_d (p + n)A$$

$\left.\vphantom{\begin{array}{c}a\\b\\c\end{array}}\right\}$ Current equations

$$\frac{\partial n}{\partial t} = \frac{-1}{Aq} \frac{\partial I_n}{\partial x} + \alpha v_d (n + p) \qquad (1)$$

$$\frac{\partial p}{\partial t} = \frac{1}{Aq} \frac{\partial I_p}{\partial x} + \alpha v_d (n + p) \qquad (2)$$

$\left.\vphantom{\begin{array}{c}a\\b\end{array}}\right\}$ Continuity equations

where I_p and I_n are the currents due to holes and electrons, respectively; q is the electronic charge; v_d is the scattering-limited drift velocity; α is the ionization coefficient for both holes and electrons, and A is the cross-sectional area of the diode. Adding Eqs. 1 and 2 and integrating from $x = 0$ to $x = \ell_a$ yields

$$\frac{dI}{dt} = - \frac{1}{\tau_a} \left[I_n - I_p \right]_{x=0}^{x=\ell_a} + \frac{2}{\tau_a} I \int_0^{\ell_a} \alpha dx,$$

where $\tau_a = \ell_a/v_d$ is the transit time across the avalanche zone. The boundary conditions at $x = 0$ and $x = \ell_a$ are indicated in Figure 5(a). At $x = 0$, the electron current is due to the reverse saturation current I_{ns} of electrons generated in the p^+ region and moved to the junction by diffusion. Thus, at $x = 0$, it follows that $I_n - I_p = 2I_n - I = 2I_{ns} - I$. At $x = \ell_a$, the hole current consists of the reverse saturation current I_{ps} of holes generated both in the n and n^+ regions so that $I_n - I_p = I - 2I_p = I - 2I_{ps}$. Therefore,

$$\frac{dI}{dt} = \frac{2I}{\tau_a} \left[\int_0^{\ell_a} \alpha dx - 1 \right] + \frac{2I_s}{\tau_a} , \qquad (3)$$

19

where $I_s = I_{ns} + I_{ps}$ is the total reverse saturation current of the diode. In an optically illuminated IMPATT diode, the reverse saturation current is greatly enhanced due to optical excitation, while in an ordinary diode, I_s is caused by thermally generated carriers and is negligible.

Eq. 3 can be simplified by replacing α by $\bar{\alpha}$, the average value of α in the avalanche zone:

$$\frac{dI}{dt} = \frac{2I \, (\bar{\alpha} \ell_a - 1)}{\tau_a} + \frac{2I_s}{\tau_a} \qquad (4)$$

Next, we introduce the small-signal approximation:

$$\bar{\alpha} = \bar{\alpha}_a + \bar{\alpha}_a' \epsilon_a$$

$$\bar{\alpha} \ell_a = 1 - \frac{I_s}{I_o} + \bar{\alpha}_a' \ell_a \epsilon_a$$

$$I = I_o = i_a$$

$$E_a = E_o + \epsilon_a \ ,$$

where $\bar{\alpha}_a'$ is the derivative of $\bar{\alpha}_a$ with respect to the electric field; E_o is the dc field; I_o is the dc current; and ϵ_a and i_a are small-signal quantities. Substituting the above equations into Eq. 4 and neglecting products of small terms leads to

$$\frac{di_a}{dt} = \frac{2I_o \bar{\alpha}_a' \epsilon_a \ell_a}{\tau_a} - \frac{2i_a I_s}{\tau_a I_o} \ . \qquad (5)$$

20

If we assume that the ac field has time dependence of $e^{j\omega t}$, it follows that

$$i_a = \frac{2\overline{\alpha}_a' \ell_a I_o \varepsilon_a}{j\omega\tau_a + \frac{2I_s}{I_o}} \cdot$$

This is the ac avalanche conduction current in the avalanche zone. The displacement current in this region is given by

$$i_{da} = j\omega\varepsilon\varepsilon_a A ,$$

where A is the cross-sectional area of the diode, and ε is the dielectric constant of the material. Thus, the total ac current I_a is

$$I_a = i_a + i_{da} = \left(\frac{j\omega\varepsilon A}{\ell} + \frac{2\overline{\alpha}_a' I_o}{j\omega\tau_a + \frac{2I_s}{I_o}} \right) \varepsilon_a \ell_a .$$

We can approximate $\varepsilon_a \ell_a$ as the ac voltage appears across the avalanche zone, so that the total ac impedance of the avalanche zone is

$$Z_a = \frac{\varepsilon_a \ell_a}{I_a} = \frac{1}{j\omega C_a + \frac{1}{j\omega L_a + R_a}} ,$$

where

$$C_a = \frac{\varepsilon A}{\ell_a}$$

21

$$L_a = \frac{\tau_a}{2\overline{\alpha}_a' I_o}$$

$$R_a = \frac{I_s}{\overline{\alpha}_a' I_o^2}$$

$$\frac{1}{L_a C_a} = \frac{2\overline{\alpha}_a' \ell_a I_o}{\varepsilon A \tau_a} \equiv \omega_a^2 \quad .$$

An equivalent circuit of the avalanche zone can be represented as a capacitor in parallel with the series combination of an inductor and a resistor, as shown in Figure 6. Define the factor D as

$$D = \frac{i_a}{I_a} = \frac{1}{\left(1 - \frac{\omega^2}{\omega_a^2}\right) + j \frac{2 I_s \omega}{\tau_a I_o \omega_a^2}} \quad . \tag{6}$$

The fact that D is complex indicates that there is a phase shift between the avalanche current and the total ac current due to the optically generated reverse saturation current I_s. Also the existence of R_a in the equivalent circuit lowers the Q of the avalanche zone. The magnitude of R_a is directly proportional to the saturation current I_s. In an ordinary IMPATT diode, $I_s \ll I_o$ and therefore

$$R_a \approx 0$$

and

$$D = \frac{1}{1 - \frac{\omega^2}{\omega_a^2}} \quad \text{(a real number)}.$$

22
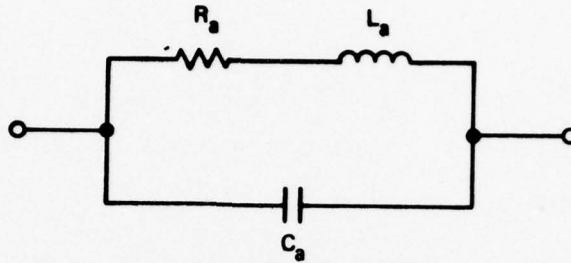
$$R_a = \frac{I_s}{\bar{\alpha}_a{}' I_o{}^2}$$

$$L_a = \frac{\tau_a}{2\,\bar{\alpha}_a{}' I_o}$$

$$C_a = \frac{\epsilon A}{\ell_a}$$

Figure 6. Equivalent circuit of the avalanche zone of an optically illuminated IMPATT diode.

We can also express Z_a in terms of D by using

$$i_{da} = I_a(1 - D)$$

$$i_{da} = j\omega\epsilon\epsilon_a A$$

$$\epsilon_a = \frac{I_a(1 - D)}{j\omega\epsilon A}$$

$$v_a = \epsilon_a \ell_a = \frac{I_a(1 - D)}{\frac{j\omega\epsilon A}{\ell_a}} = \frac{I_a(1 - D)}{j\omega C_a} \,,$$

23

from which it follows that

$$Z_a = \frac{v_a}{I_a} = \frac{1 - D}{j\omega C_a} \; . \tag{7}$$

B. THE DRIFT ZONE

Once the avalanche current enters the drift zone, it propagates as an unattenuated current wave at scattering-limited velocity v_d:

$$i_c(x) = i_a e^{-j\omega \frac{x}{v_d}} = DI_a e^{-j\omega \frac{x}{v_d}} \; .$$

Again, the total ac current is $I_d = i_c + i_d$, where i_d is the displacement current in the drift zone:

$$i_d = j\omega \epsilon \epsilon_d A$$

and therefore

$$I_d = DI_a e^{-j\omega \frac{x}{v_d}} + j\omega \epsilon \epsilon_d A$$

and

$$\epsilon_d = I_d \frac{1 - De^{-j\omega \frac{x}{v_d}}}{j\omega \epsilon A} \; , \tag{8}$$

24

where we used the fact that $I_a = I_d$. Integrating Eq. 8 from $x = 0$ to $x = \ell_d$, assuming $\ell_d \gg \ell_a$, yields

$$V_d = \frac{I_d \ell_d}{j\omega\varepsilon A}\left[1 - D\;\frac{1 - e^{-j\theta}}{j\theta}\right]\;, \tag{9}$$

where

$$\theta = \omega\tau_d = \omega\,\frac{\ell_d}{v_d}\;.$$

The ac impedance of the drift zone is

$$Z_d = \frac{V_d}{I_d} = \frac{1 - D}{j\omega C_d} + \frac{D}{j\omega C_d}\left(1 - \frac{\sin\theta}{\theta}\right) + \frac{D\theta}{2\omega C_d}\left(\frac{1 - \cos\theta}{\frac{\theta^2}{2}}\right)\;,$$

where

$$C_d = \frac{\varepsilon A}{\ell_d}\;.$$

For small transit angle, $\theta \ll 1$, it follows that

$$\frac{\sin\theta}{\theta} \approx 1 \text{ and } \frac{1 - \cos\theta}{\frac{\theta^2}{2}} \approx 1\;,$$

and therefore that

$$Z_d = \frac{1 - D}{j\omega C_d} + \frac{D\theta}{2\omega C_d}\;. \tag{10}$$

25

C.   THE TOTAL IMPEDANCE

The total ac impedance of the IMPATT diode is obtained by adding Eqs. 7 and 10:

$$Z = Z_a + Z_d = \frac{1 - D}{j\omega C_a} + \frac{1 - D}{j\omega C_d} + \frac{D\theta}{2\omega C_d}$$

$$= \frac{1 - D}{j\omega C} + \frac{D\theta}{2\omega C_d} , \qquad (11)$$

where

$$\frac{1}{C} = \frac{1}{C_a} + \frac{1}{C_d} .$$

From this total small-signal impedance, we can calculate the cut-off frequency, the frequency at which the real part of the impedance vanishes.   For simplicity, we write

$$D = \frac{1}{a + jb} = \frac{a - jb}{a^2 + b^2} ,$$

where

$$a = 1 - \frac{\omega^2}{\omega_a^2} ,$$

$$b = \frac{2I_s\omega}{\tau_a I_o \omega_a^2} .$$

26

Then it follows that

$$1 - D = \frac{(a^2 + b^2 - a) + jb}{a^2 + b^2} \; .$$

The real part of the impedance can be written as

$$\text{Re}(z) = \frac{b}{\omega c (a^2 + b^2)} + \frac{\tau_d a}{2 C_d (a^2 + b^2)} \; .$$

Setting $\text{Re}(z) = 0$ yields

$$\frac{b}{\omega c} + \frac{\tau_d a}{2 C_d} = 0$$

$$\omega^2 - \omega_a^2 = \frac{4 I_s C_d}{\tau_a \tau_d C I_o} \; .$$

Recall that

$$C_d = \frac{\varepsilon A}{\ell_d}$$

$$C_a = \frac{\varepsilon_a}{\ell_a}$$

$$C = \left(\frac{1}{C_a} + \frac{1}{C_d} \right)^{-1} = \frac{C_a C_d}{C_a + C_d}$$

because

$$\ell_d \gg \ell_a, \; C_a \gg C_d \; .$$

27

Therefore it follows that

$$C \approx C_d$$

and

$$\omega^2 = \omega_a^2 + \frac{4I_s}{\tau_a \tau_d I_o}$$

or

$$\omega_c^2 = \omega_a^2 + \omega_s^2$$

where

$$\omega_s^2 = \frac{4I_s}{\tau_a \tau_d I_o} , \qquad\qquad (12)$$

We can also calculate the resonance frequency, that is, the frequency at which the imaginary part of the impedance vanishes:

$$Im(z) = -j\frac{(a^2 + b^2 - a)}{\omega c} \frac{1}{a^2 + b^2} + \frac{\tau_d}{2C_d}\left(\frac{-jb}{a^2 + b^2}\right) .$$

Setting $Im(z) = 0$ yields

$$\frac{a^2 + b^2 - a}{\omega c} + \frac{\tau_d b}{2C_d} = 0 .$$

28

Again, since

$$C \approx C_d ,$$

it follows that

$$\omega^2 = \omega_R^2 = \omega_a^2 \left(1 - \frac{\tau_d I_s}{\tau_a I_o}\right) - \frac{4I_s^2}{\tau_a^2 I_o^2} .$$

Thus, the cutoff frequency ω_c and the resonance frequency ω_R of an IMPATT diode under optical illumination are different in general. In the absence of light, $I_s \ll I_o$ and $\omega_R = \omega_c = \omega_a$. Moreover, ω_c increases with increasing I_s while ω_R decreases with increasing I_s. It is the strong dependence of ω_c and ω_R on illumination that results in the switching phenomena observed in IMPATT diode oscillators. The calculated results and the experimental results are discussed in the next section.

29

SECTION 4

DISCUSSION AND COMPARISON OF THE CALCULATED AND
EXPERIMENTAL RESULTS

It is instructive to first examine the frequency dependence of the IMPATT diode impedance without optical illumination. The expression of total impedance of the diode derived earlier also can be applied to the case of no illumination. From Eqs. 7 and 11, setting $I_s = 0$, we have

$$D = \frac{1}{1 - \dfrac{\omega^2}{\omega_a^2}}$$

$$1 - D = \frac{1}{1 - \dfrac{\omega_a^2}{\omega^2}}$$

$$Z = \frac{-j}{\omega C} \; \frac{1}{1 - \dfrac{\omega_a^2}{\omega^2}} + \frac{\tau_d}{2C_d} \; \frac{1}{1 - \dfrac{\omega^2}{\omega_a^2}}$$

and hence

$$R = \mathrm{Re}(Z) \approx \frac{\tau_d}{2C_d} \; \frac{1}{1 - \dfrac{\omega^2}{\omega_a^2}} \tag{13}$$

$$X = \mathrm{Im}(Z) \approx \frac{-1}{\omega C} \; \frac{1}{1 - \dfrac{\omega_a^2}{\omega^2}} \; . \tag{14}$$

31

A plot of $R(\omega)$ and $X(\omega)$ is shown in Figure 7. When $\omega > \omega_a$, the real part of the diode impedance is negative, and the imaginary part is capacitive; for $\omega < \omega_a$, the opposite is true. We will use a simple series inductance to illustrate the tuning and oscillation condition of the diode. The reactance of a series inductor L is ωL. We plot the negative of this quantity on the impedance versus frequency diagram of the IMPATT diode so that the intersection of this curve with the reactance curve of the diode determines the oscillation frequency ω_o. A vertical projection from the intersection to the resistance curve shows the value of negative resistance available at this frequency. This negative resistance has to be large enough to overcome the loss in the microwave cavity and in the diode itself for oscillation to sustain. For example, as illustrated in Figure 7, with inductance L_1 the available negative resistance is R_1, which is above the threshold value R_{th}, and the device will oscillate at frequency ω_o. However, if the inductance is changed to L_2, then the magnitude of the negative resitance available is only R_2, which is below R_{th}, hence the device will not oscillate at ω_o'.

Next, we examine the frequency dependence of the IMPATT diode impedance subject to optical illumination. Again, we use Eqs. 7 and 11. With the approximation $C \approx C_d$, we can derive

$$R = \text{Re}(Z) = \frac{\tau_d}{2C_d}\, \omega_a^2\, \frac{\omega_a^2 + \omega_s^2 - \omega^2}{\left(\omega_a^2 - \omega^2\right)^2 + \left(\dfrac{\tau_d \omega_s^2}{2}\right)^2 \omega^2} \tag{15}$$

$$X = \text{Im}(Z) = \frac{-1}{\omega C}\, \frac{\omega^2 \left[\omega^2 - \omega_a^2 \left(1 - \dfrac{\tau_d^2 \omega_s^2}{4}\right)^2 + \left(\dfrac{\tau_d \omega_s^2}{2}\right)^2\right]}{\left(\omega_a^2 - \omega^2\right)^2 + \left(\dfrac{\tau_d \omega_s^2}{2}\right)^2 \omega^2}, \tag{16}$$
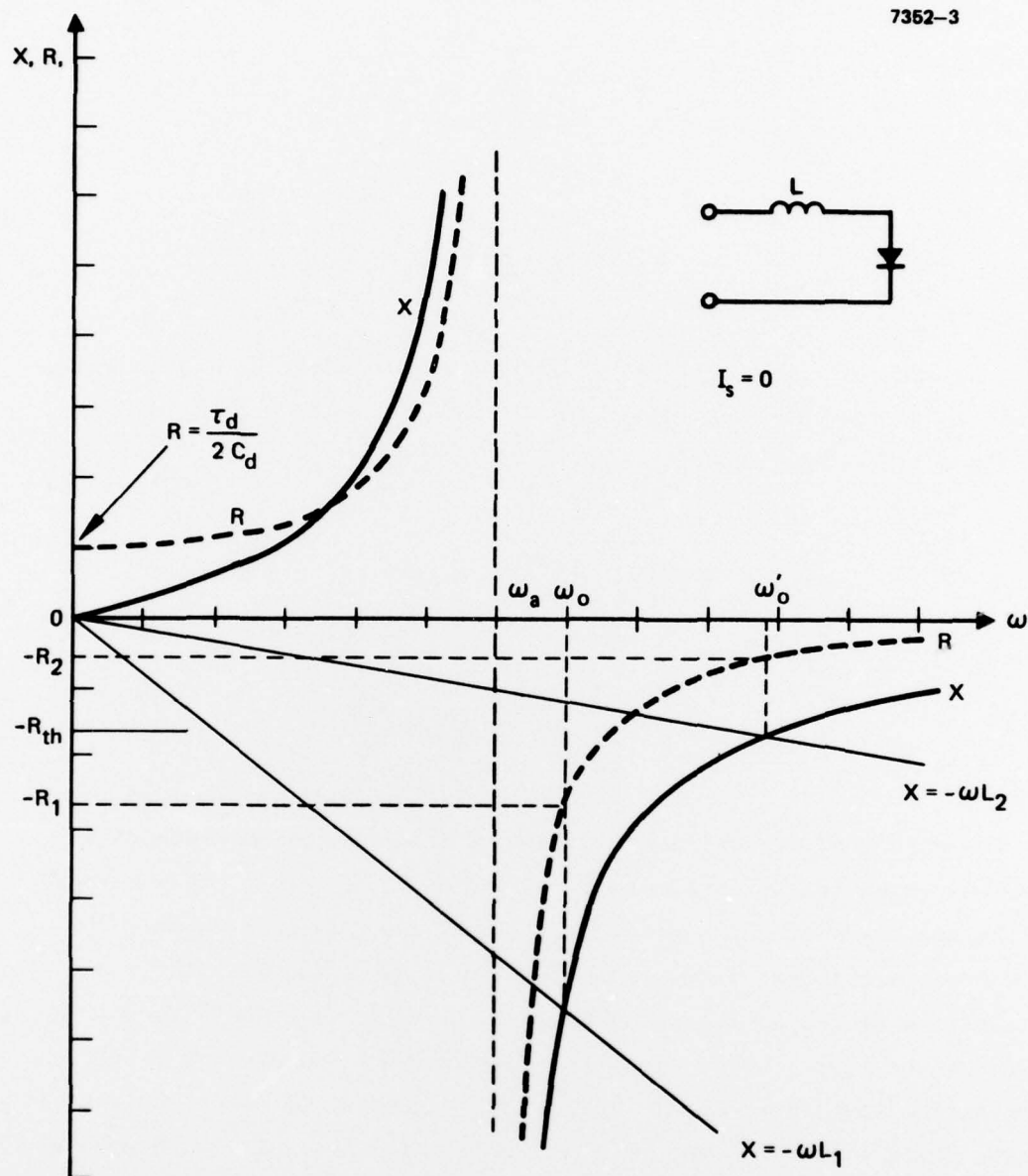
Figure 7. Impedance versus frequency plot of an IMPATT diode.

where

$$\omega_a^2 = \frac{2\overline{\alpha}_a \ell_a I_o}{\varepsilon A \tau_a}$$

$$\omega_s^2 = \frac{4 I_s}{\tau_a \tau_d I_o}$$

In the absence of optical illumination, $\omega_s = 0$ and Eqs. 15 and 16 reduce to Eqs. 13 and 14, respectively. Eqs. 15 and 16 are sketched in Figures 8 and 9 for the case of

$$\frac{\tau_d}{2} = \frac{1}{\omega_a}$$

$$\omega_s^2 = \frac{\omega_a^2}{10} \quad , \quad \frac{\omega_a^2}{20} \quad , \quad \text{and} \quad \frac{\omega_a^2}{30} \quad .$$

The effect of optical illumination on the negative resistance of the diode is obvious from Figure 8. Singularity at $\omega = \omega_a$ is removed, and the magnitude of the negative resistance is greatly reduced. The R = 0 frequency as we calculated before is larger than ω_a. The reactance of the diode, as shown in Figure 9, is also modified. For $\omega > \omega_a$, the reactance curves shift slightly toward higher frequencies as the illumination level increases. This small shift is important because, it changes the oscillation frequency. A detailed drawing of the negative resistance and reactance at $\omega > \omega_a$ is shown in Figure 10 for the case of no optical illumination and for the case when

$$\omega_s^2 = \frac{\omega_a^2}{10} \quad .$$

34

$$\frac{\tau_d}{2} = \frac{1}{\omega_a}$$

$$\omega_s^2 = \frac{\omega_a^2}{10}$$

$$\omega_s^2 = \frac{\omega_a^2}{20}$$

$$\omega_s^2 = \frac{\omega_a^2}{30}$$

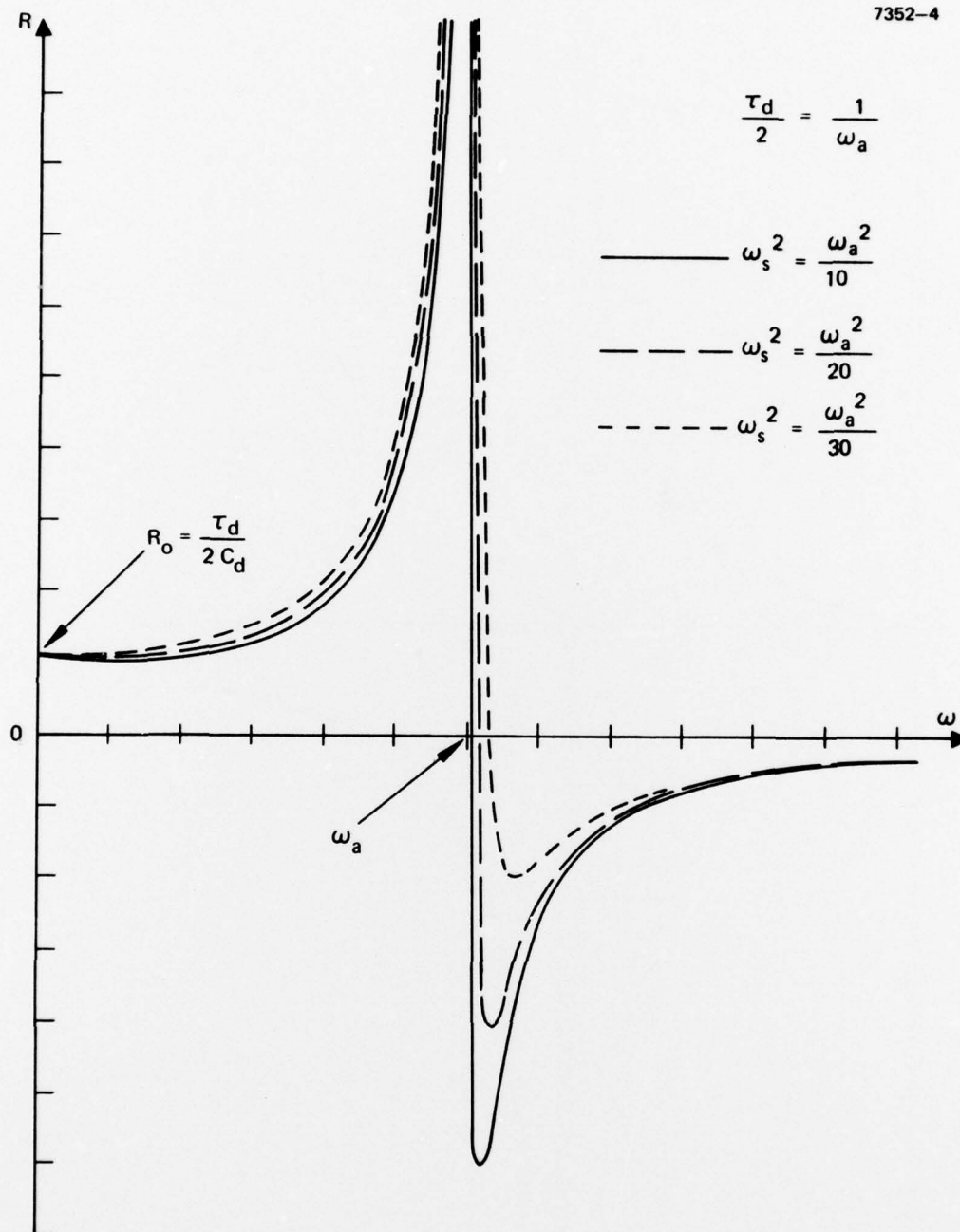$$R_o = \frac{\tau_d}{2\,C_d}$$

ω_a

Figure 8. Frequency dependence of the real part of the IMPATT diode impedance subject to optical illumination.
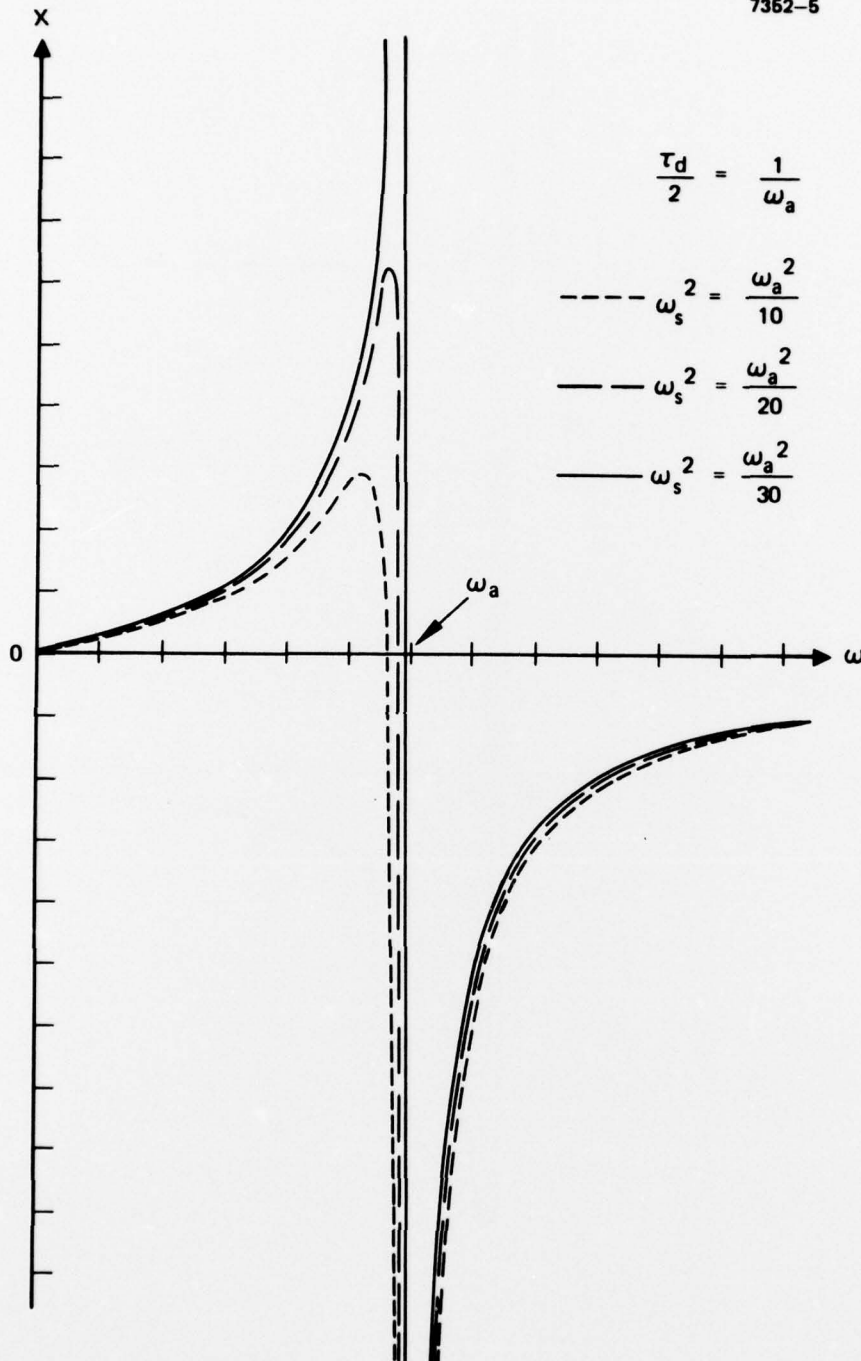
Figure 9. Frequency dependence of the imaginary part of the IMPATT diode impedance subject to optical illumination.
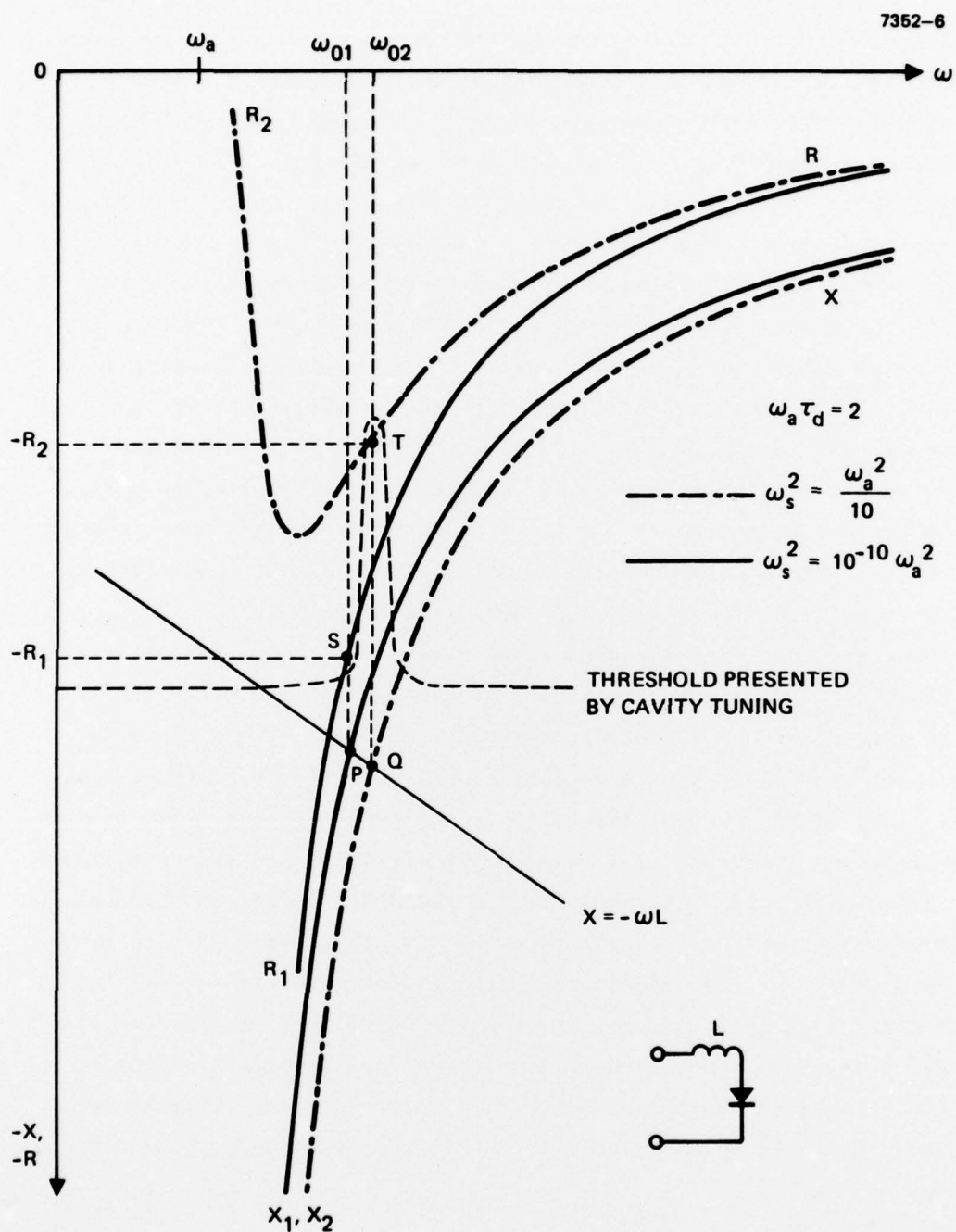
Figure 10. Determination of oscillation frequency of an IMPATT oscillator with and without illumination.

Again, the diode is in series with an inductor L to complete the circuit, and the negative of this inductance is shown by the straight line $X = -\omega L$. This line intersects the reactance curve X_1 at P, which determines the oscillation frequency ω_{01} and the magnitude of the negative resistance $-R_1$ available. If the cavity is tuned to this frequency and $-R_1$ exceeds the threshold value, then the IMPATT diode will oscillate. Now assume that an intense optical pulse is applied to the diode such that the X_1 curve is shifted to X_2 and the R_1 curve is changed to R_2. Once again, the intersection of the $X = -\omega L$ line and the X_2 curve, Q, determines the new "would be" oscillation frequency ω_{02} and the available negative resistance $-R_2$. Since $|R_1| > |R_2|$, the diode will oscillate with reduced output power if $-R_2$ is above threshold value at frequency ω_{02}, or it will cease oscillation if $-R_2$ is below threshold. This case corresponds to the experimental results shown in Figure 3. If the cavity is tuned carefully, we could have a frequency-dependent oscillation threshold, as shown by the dashed curve. With this threshold situation, the IMPATT diode will not oscillate without illumination since the negative resistance at ω_{01} is below threshold. However, if the diode is illuminated with the proper amount of light, it will oscillate at frequency ω_{02}. If the optical intensity is increased further, the "would be" oscillation frequency will be even higher, which has negative resistance below threshold, and therefore the oscillation will be quenched. This case corresponds to the experimental results shown in Figure 4.

Thus, the observed experimental results described in Section 2 can be understood qualitatively through the calculated results and the mechanisms discussed above. However, we must realize that, although the output power of the IMPATT diode oscillator is being switched or modulated, there is an oscillator frequency change associated with the process.

SECTION 5

PLANS FOR THE NEXT QUARTER

In the next quarter, we will continue the theoretical portion of the program with particular emphasis on the optical injection-locking of solid-state oscillators. We will examine the efficiency of injection locking caused by the various order of subharmonics, the effect of frequency noise associated with the reference signal on the locked oscillator output; and the long-term stability of the optical injection-locking scheme. The results of this study will determine the feasibility of locking millimeter-wave oscillators through optical injection. The optical response of GaAs FETs will be modeled to understand the optical injection locking, mixing, and frequency noise reduction in this device.

Experimentally, we will continue the effort to determine the noise figure of the GaAs FET amplifier as a microwave mixer. Also, we will carry out optical injection locking of an IMPATT diode oscillator.

REFERENCES

1. W. T. Read, Jr., Bell Syst. Tech. J., 37, 401 (1958)

2. G. I. Haddad, P. T. Greiling, and W. E. Schroeder, IEEE Trans. MIT, 18, 752 (1970).

3. S. M. Sze, and R. M. Ryder, Proc. IEEE, 59, 1140 (1971).

4. S. M. Sze, Physics of Semiconductor Devices, New York, Wiley, 1969.

5. M. Gilden and M. E. Hines, IEEE Trans. Electron. Devices, ED-13, 169 (1966).

6. A. C. Sanderson and A. G. Jordan, Solid-State Electronics, 15, 140 (1972).